

# Bioactive Unnatural Somatostatin Analogues through Bioorthogonal Iodo- and Ethynyl-Disulfide Intercalators

Anne Pfisterer,<sup>[b]</sup> Klaus Eisele,<sup>[a, b]</sup> Xi Chen,<sup>[a]</sup> Manfred Wagner,<sup>[b]</sup> Klaus Müllen,<sup>[b]</sup> and Tanja Weil\*<sup>[a]</sup>

**Abstract:** Iodo- and ethynyl-containing bisalkylating bioconjugation agents **5** and **8** were achieved and allow the introduction of reactive unnatural substituents into proteins and peptides whilst the bioactive 3D structure is retained. Derivatives of the peptide hormone somatostatin bearing a single iodo or ethynyl group were prepared through intercalation into the disulfide bridge. For the first time, the exact reaction mechanism of the intercalation was elucidated by applying 2D NMR experiments and it was shown that, during the reaction, somatostatin dia-

stereomers were formed. Site-directed modification of the ethynyl-modified peptide with a coumarin chromophore was achieved through a [1,3] dipolar Huisgen cycloaddition reaction; this suggests that such a derivative could serve as an attractive platform to prepare artificial somatostatin compound libraries. The biological activity and specificity of a representative modified

somatostatin derivative was demonstrated and efficient receptor-mediated cell uptake occurred in a dose-dependent manner into receptor positive cells only. The iodo and ethynyl bioconjugation reagents presented herein could be applied for introducing such substituents into alternative peptides and proteins and, in principle, could facilitate the efficient design of a broad variety of artificial protein and peptide analogues with previously unknown bioactivities.

**Keywords:** antitumor agents • bio-organic chemistry • intercalations • Michael addition • peptides

## Introduction

Protein- or peptide-based drugs are emerging therapeutics that combine high biological activities, biocompatibilities, and specificities. However, their pharmacokinetic profile often represents a major limitation that makes their preclinical and clinical development challenging.<sup>[1]</sup> Therefore, a wide range of posttranslational modifications have been explored in order to improve their proteolytic stability, membrane and tissue penetration, and oral and bioavailability.<sup>[2,3]</sup> Up to now, only a few chemistry approaches have been reported that allow the introduction of functional groups at a specific location on the protein surface or into the peptide backbone in a reproducible fashion. Tailored reagents, as well as enzymes, have been applied to specifically modify the N terminus of proteins,<sup>[4–6]</sup> and cysteine point mutations allowing site-directed modifications<sup>[7–9]</sup> or noncanonical

amino acids bearing bioorthogonal groups such as ethynyl groups<sup>[10,11]</sup> have successfully been introduced. However, the main challenges of these approaches include low product yields or the loss of bioactivity after modification or mutagenesis.

In this context, it has been shown that the intercalation of tailored alkylation agents into native disulfide bonds provides an efficient way to selectively modify biomolecules.<sup>[12]</sup> Up to now, mainly poly(ethylene oxide) chains have been attached to antibodies or Fab fragments<sup>[13]</sup> in a site-directed fashion. From the inspiration of these published bisalkylating reagents, two bithiol-reactive labels bearing a single bioorthogonal ethynyl or iodo group have been designed. Bioorthogonality is essential to target only one functionality, regardless of the presence of other functional groups in the amino acid side chains.

We have selected the cyclic tetradecapeptide somatostatin-14, due to its important biological role, its relatively small size, and the presence of only a single disulfide bond.<sup>[14]</sup> Somatostatin is a hormonal neuropeptide that was found to inhibit growth-hormone secretion from the pituitary gland<sup>[15]</sup> and that also plays a decisive role in other physiological functions, including the inhibition of gastric release, insulin, glucagon, and various intestinal hormones.<sup>[16]</sup> In addition, several cancer cells, such as endocrine tumors like pancreatic tumors, express a specific class of somatostatin receptors in their cell membranes, which thus facilitates somatostatin uptake through receptor-mediated endocytosis.<sup>[15,17]</sup> Therefore, radiolabeled somatostatin derivatives

[a] Dr. K. Eisele, X. Chen, Prof. Dr. T. Weil  
Institute of Organic Chemistry III  
University of Ulm  
Albert-Einstein-Allee 11, 89069 Ulm (Germany)  
Fax: (+49) 731-5022883  
E-mail: Tanja.Weil@uni-ulm.de

[b] A. Pfisterer, Dr. K. Eisele, Dr. M. Wagner, Prof. Dr. K. Müllen  
Max Planck Institute for Polymer Research  
Ackermannweg 10, 55128 Mainz (Germany)

Supporting information for this article is available on the WWW under <http://dx.doi.org/10.1002/chem.201100287>.

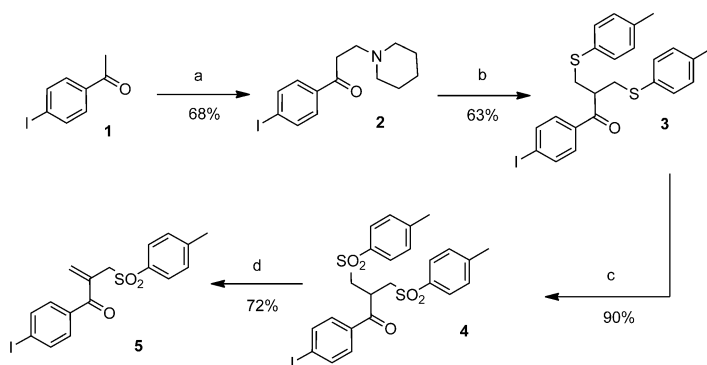
have been used as attractive diagnostic tools for identifying and imaging certain cancer cells.<sup>[18]</sup>

The biological activity of somatostatin originates from the loop sequence Phe<sup>7</sup>-Trp<sup>8</sup>-Lys<sup>9</sup>-Thr<sup>10</sup>, which is crucial for high-affinity G-protein-coupled membrane receptor uptake.<sup>[19]</sup> This loop is maintained by Cys<sup>3</sup> and Cys<sup>14</sup> forming a disulfide bridge, which is essential to maintain biological integrity.<sup>[20]</sup> Unfortunately, somatostatin has a very low plasma stability of only a few minutes<sup>[21]</sup> due to disulfide cleavage, which greatly limits its medicinal applications. Therefore, a few synthetic somatostatin analogues with longer plasma stability, such as octreotide, have been prepared.<sup>[15,22–24]</sup> The preparation of bioactive somatostatin derivatives bearing unnatural functionalities might reveal unusual *in vivo* bioactivities, as well as an altered pharmacokinetic profile, which could be attractive for the design of improved somatostatin drug conjugates.

Herein, the design and synthesis of iodo- and ethynyl-containing intercalation agents, the intercalation mechanism into the disulfide bridge of somatostatin, and the bioactivity of the synthesized derivatives will be discussed. Such novel bioorthogonal conjugation reagents offer an attractive platform for the introduction of desirable artificial substituents into peptides and proteins and thus offer an efficient alternative for reproducible and site-directed protein modifications.

## Results and Discussion

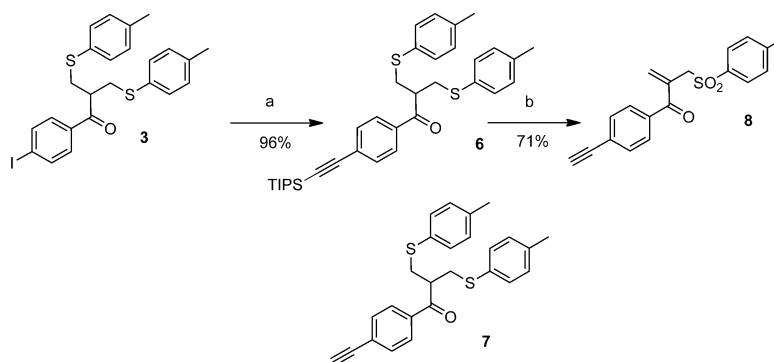
**Synthesis of bioorthogonal iodo- and ethynyl-functionalized intercalation reagents:** The introduction of iodo substituents is attractive because high-yield palladium(0)-catalyzed cross-coupling reactions, such as the Heck, Suzuki, or Sonogashira reactions,<sup>[25]</sup> allow a broad range of further chemical modifications. Due to recent success in synthesizing ligands that allow palladium-catalyzed reactions in water, we have designed a synthetic pathway towards the iodo-containing monosulfone protein or peptide intercalator **5**, as outlined in Scheme 1. Compound **5** was prepared from *p*-iodoacetophenone (**1**) in a four-step synthesis. First, preparation of the Mannich salt **2** proceeded in the presence of piperidine hydrochloride and paraformaldehyde with acceptable yields. Thereafter, **2** was treated with 4-methylbenzenethiol, piperidine, and formalin to yield the iodo-bis-sulfide **3**. Compound **3** was further oxidized to the iodo-bis-sulfone **4** and, after elimination of *p*-toluene sulfinic acid with potassium *tert*-butoxide, the iodo-functionalized monosulfone **5** was isolated in acceptable yields (Scheme 1).



Scheme 1. Synthesis of iodo-functionalized monosulfone reagent **5**. a) Piperidine HCl, HCl, paraformaldehyde, EtOH, 105°C; b) piperidine, formalin, 4-methylbenzenethiol, EtOH, 105°C; c) oxone, EtOAc/CH<sub>3</sub>CN/H<sub>2</sub>O; d) KO<sup>t</sup>Bu, tetrahydrofuran (THF).

In addition, the triisopropylsilyl (TIPS) protected ethynyl-bis-sulfide **6** was obtained in excellent yields from iodo-bis-sulfide **3** by treatment with TIPS acetylene in the presence of PdCl<sub>2</sub>(PPh<sub>3</sub>) and Cu<sub>2</sub>I<sub>2</sub> (Scheme 2). As the deprotected ethynyl-bis-sulfide **7** was highly sensitive to the presence of oxygen, it was advisable to perform the oxidation of the sulfide groups prior to removal of the TIPS protecting group. The highly basic system generated by the addition of TBAF to the oxidized TIPS-protected ethynyl-bis-sulfide **6** dissolved in THF facilitated the deprotection of the ethynyl group and, at the same time, the elimination of *p*-toluene sulfinic acid to afford the ethynylmonosulfone **8** in one reaction step only (Scheme 2).

The intercalating reagents iodomonosulfone **5** and ethynylmonosulfone **8** both allow covalent modification of native disulfide bonds through reductive liberation of the cysteine thiol groups or the introduction of bioorthogonal reactive groups suitable for bioconjugation reactions, even in the presence of unprotected amino acid residues. These tailored organic molecules provide an attractive platform with novel bioorthogonal tags that could be further treated with a broad range of reagents in a highly selective fashion.



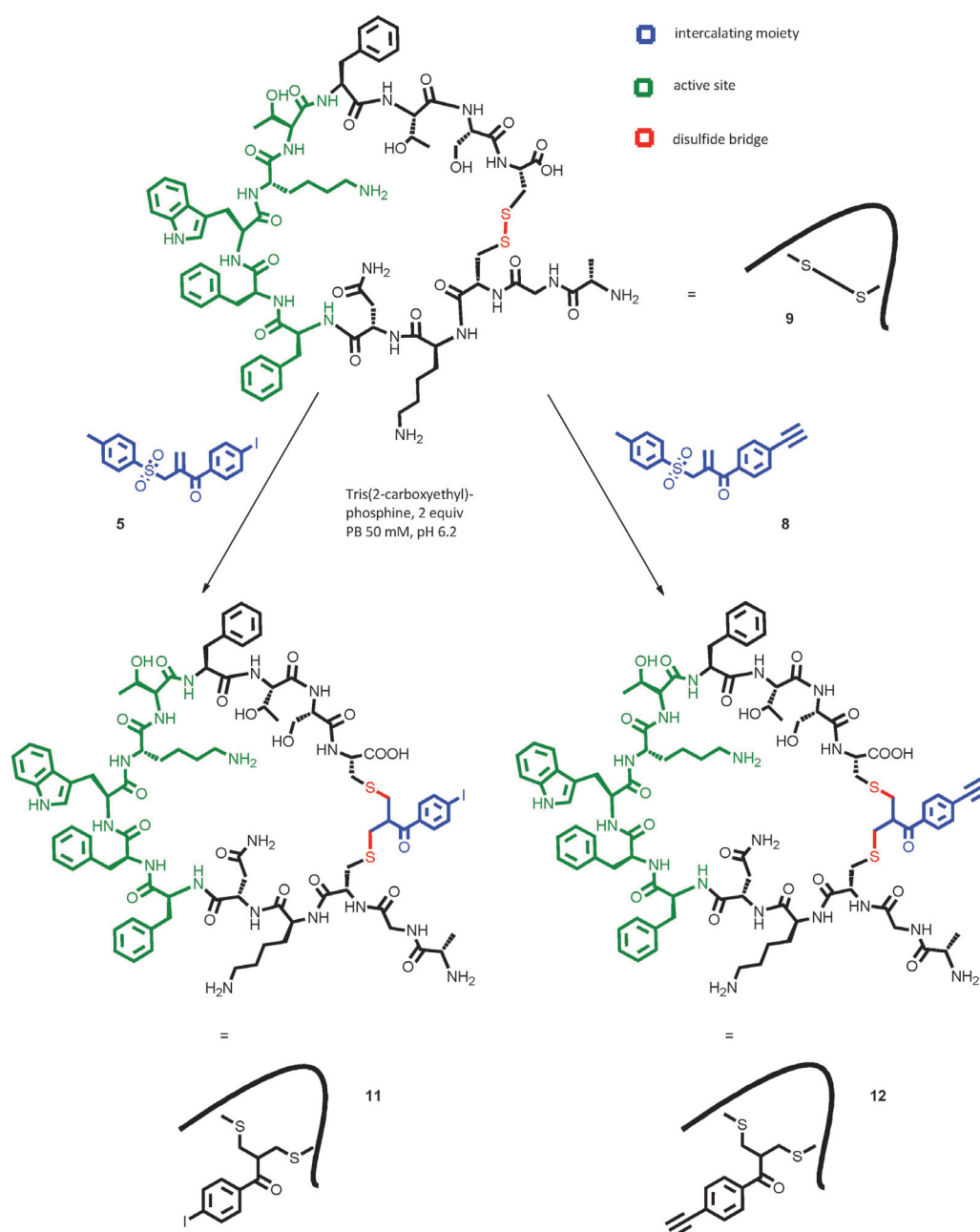
Scheme 2. Synthesis of ethynyl-functionalized monosulfone reagent **8**. a) Triisopropylsilylacetylene, copper(I) iodide, PdCl<sub>2</sub>(PPh<sub>3</sub>)<sub>2</sub>, THF/Et<sub>3</sub>N; b) 1. oxone, dichloromethane, 2. tetrabutylammonium fluoride (TBAF), THF.

**Bioorthogonal functionalized somatostatin derivatives:** Somatostatin represents an ideal model peptide for assessing the potential of both bioorthogonal intercalation agents **5** and **8** because 1) only a single disulfide group is present for chemical modification, 2) reaction control and product and side-product characterization could be realized through mass spectrometry and NMR spectroscopy due to the small size of the peptide, and 3) preservation of the bioactive 3D conformation could be accessed through suitable cell models.

As described above, somatostatin bears a single disulfide bridge that is essential for biological activity. Therefore, modification of this disulfide bridge by intercalation of **5**

and **8** with retention of the 3D geometry represents a key concern. The disulfide bridge of somatostatin acetate (**9**) was first reduced by adding tris(2-carboxyethyl)phosphine hydrochloride (TCEP HCl) to form reduced somatostatin **10**, which was then conjugated to the iodomonosulfone reagent **5** to yield pure iodosomalatostatin **11** after purification by filtration and reversed-phase chromatography (Scheme 3). The corresponding ethynyl derivative **12** was obtained and purified by the same approach (see the Experimental Section).

Figure 1 reveals the analytical HPLC trace of native somatostatin **9**, reduced somatostatin **10**, and iodo-modified reduced somatostatin **11** with traces of **10**. Interestingly, the retention



Scheme 3. Synthesis of bioorthogonally functionalized somatostatins **11** and **12**.

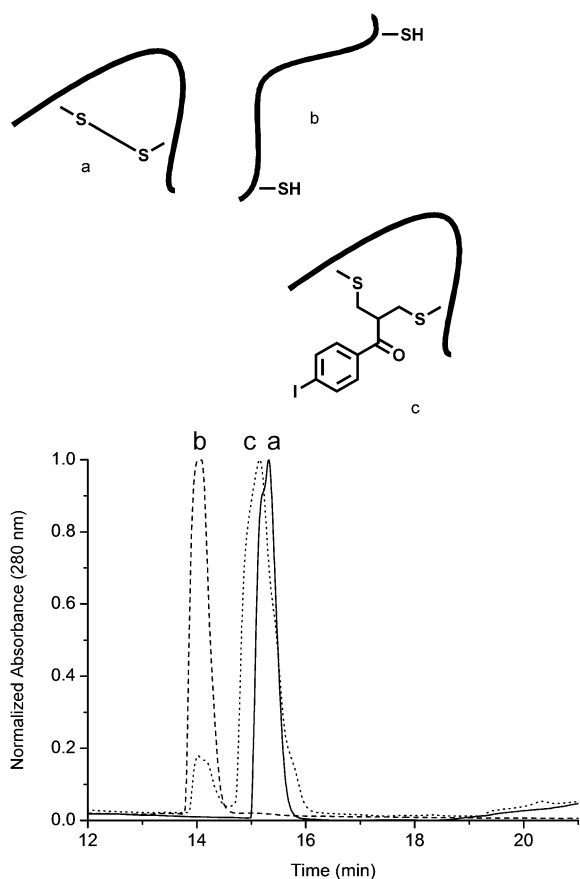


Figure 1. Illustration of the intercalation reaction by reversed-phase HPLC: Chromatograms for native somatostatin (**9**; solid line a), disulfide-reduced somatostatin **10** (dashed line b), and iodo-modified somatostatin **11** with traces of **10** (dotted line c). The two cyclic peptides (lines a and c) have similar retention times, whereas the reduced linear peptide (line b) elutes faster

times of **9** and **10** differ, whereas **9** and **11** display nearly equal retention times. This observation suggests that the cyclic structure of somatostatin was retained after modification, which is crucial for keeping the biological activity after bioconjugation.

The identities of the modified peptides **11** and **12** were also confirmed by MALDI-TOF and ESI-TOF mass spectrometry. As representative examples, the spectra of native somatostatin **9**, iodo-modified somatostatin **11**, and ethynyl-modified somatostatin **12** are shown in Figure 2.

The optimal conditions for somatostatin modification were

identified according to mass spectrometry studies with different quantities of the alkylating reagents. The use of 1.5 equivalents of ethynylmonosulfone reagent (Figure 3) yielded monosubstituted somatostatin derivative **12**, whereas traces of unmodified somatostatin **9** were also detected by MALDI-TOF mass spectrometry with the application of only 1.2 equivalents of the reagent. Higher quantities such as 2 or 3 equivalents yielded the monosulfone along with traces of the doubly substituted, linear peptide. Obviously, a second intermolecular addition reaction occurs if the bioconjugation reagent is used in excess.

The mechanism of this reaction has been suggested by Lawton and co-workers<sup>[26]</sup> as an in situ addition–elimination procedure (Scheme 4). However, this reaction mechanism has never been supported by experimental data. The first addition of the nucleophilic thiol group to the Michael acceptor system of the reagent is followed by elimination of *p*-toluene sulfonic acid to generate the second addition system (Scheme 4, top). Covalent rebridging proceeds by attack of the second thiol group. This mechanistic pathway for the cross-linking of sulfhydryl groups was proposed by Mitra and Lawton,<sup>[12]</sup> but the structural identity of the three-carbon bridge formed due to intercalation has never been proven.

Therefore, NMR studies have been undertaken in order to elucidate this reaction mechanism. After purification of iodosomatostatin **11** by reversed-phase HPLC, the conjugate was freeze-dried and different deuterated solvents were investigated for the NMR experiments. The best resolution of the signals was achieved in D<sub>2</sub>O with suppression of the HDO signal. Additionally, proton exchange of the amide and amino protons facilitated the analysis of the spectra and

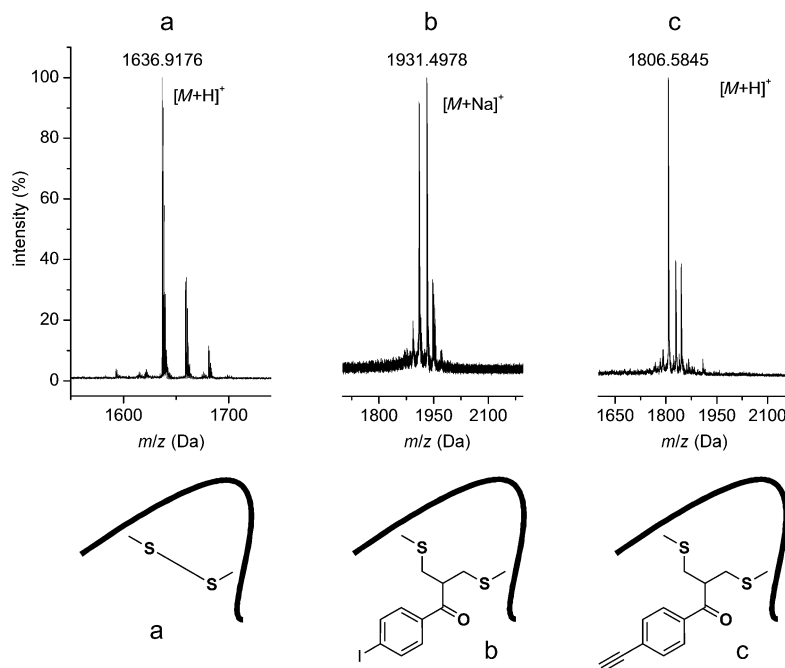


Figure 2. MALDI-TOF mass spectra: a) Native somatostatin (**9**) with its salt adducts, b) somatostatin derivative **11** after modification with the iodomonosulfone, and c) somatostatin derivative **12** after modification with the ethynylmonosulfone.

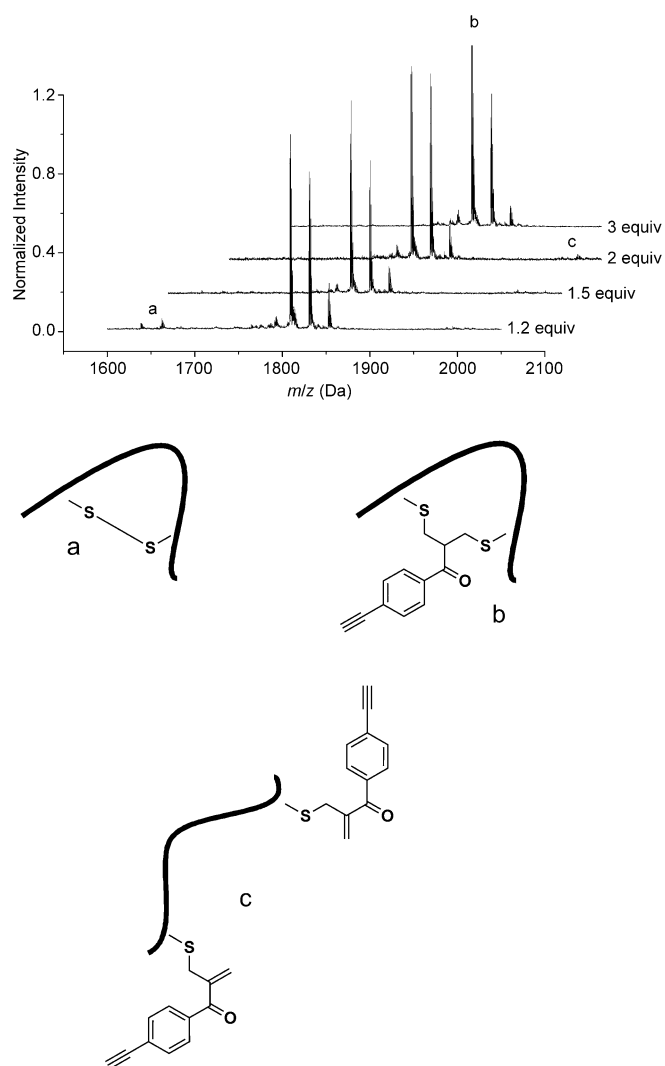


Figure 3. MALDI-TOF mass spectra of reaction mixtures of somatostatin with different amounts of ethynylmonosulfone **8**. With 1.2 equivalents, unmodified somatostatin (labeled a) is still present, whereas traces of double-labeled somatostatin (labeled c) appear with 2 or 3 equivalents of linker. With 1.5 equivalents of monosulfone linker, neither native nor double-modified somatostatin, but only the cyclic modified peptide (labeled b), were detected.

the assignment of the signals. The diastereomers are not magnetically equivalent, so the cyclic identity of the modified peptide was proven for the first time by  $^1\text{H}$  NMR techniques.

In Figure 4, the  $^1\text{H}$  NMR spectra of native somatostatin (a) and iodo-modified somatostatin (b) are compared. Whereas 2D-NMR techniques allowed

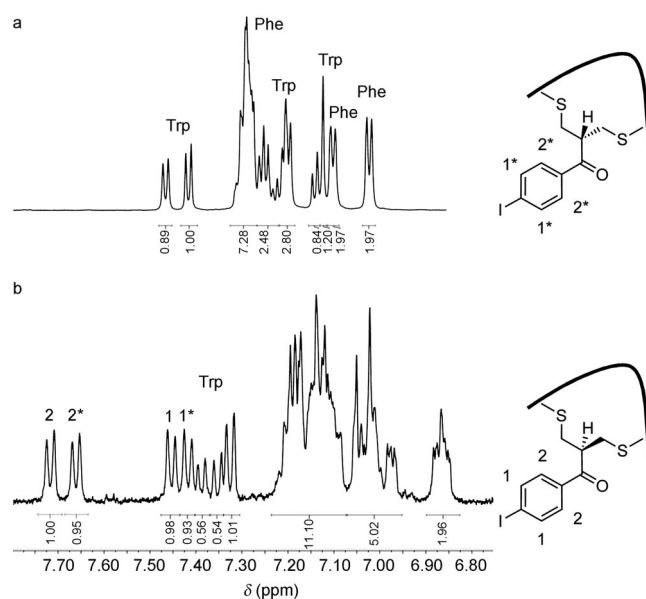
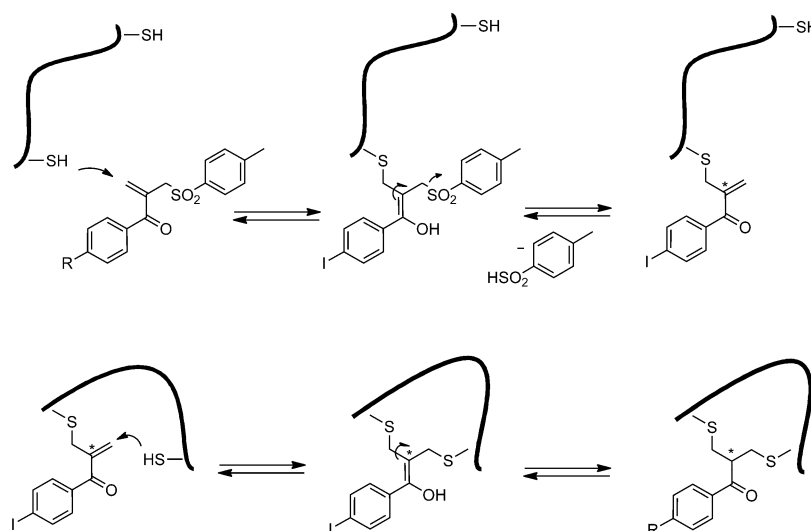


Figure 4. The formation of diastereomers of iodo-modified somatostatin **11** was confirmed by  $^1\text{H}$  NMR spectrometry. a)  $^1\text{H}$  NMR spectrum of the aromatic region of native somatostatin (**9**). b)  $^1\text{H}$  NMR spectrum of the aromatic region of iodo-modified somatostatin **11**. The relative intensities of the signals of the aromatic reagent protons of the two diastereomers of iodo-modified somatostatin **11** (1,1\* and 2,2\* in the structures, respectively) were compared to the relative intensity of all of the aromatic signals.

the signals of the aromatic protons of native somatostatin to be assigned, the elucidation of the spectrum of iodiosomatostatin **11** is much more complex due to the existence of two somatostatin diastereomers with different magnetic behaviors. Obviously, during the second addition step, a new chiral center is created due to keto–enol tautomerism of the newly generated ketone (Scheme 4). This racemization leads to the formation of diastereomers and no enantiomerically



Scheme 4. Proposed addition–elimination mechanism for the intercalation of iodomonosulfone **5** into the reduced form of somatostatin to yield iodo-functionalized somatostatin **11**. Racemization in the second addition step leads to formation of diastereomers.

pure product is obtained, which might be of great relevance because chiral centers are important in biological systems. The signals of the iodophenyl protons (H1, H1\*, H2, and H2\*; Figure 4) were assigned and their relative intensity was 1:1:1:1, whereas the ratio of the relative intensity of these protons versus the relative intensity of all aromatic signals was 1:6. This factor is consistent with the fact that conjugation provided a total of twenty-four aromatic protons and with the assumption that two diastereomers are formed in a 1:1 ratio.

In addition, the signal for the aromatic methyl group and the two signals corresponding to the nonequivalent hydrogen atoms of the double bond were no longer present in the spectrum of **11**. Moreover, the COSY cross-peaks at  $\delta=3.78$  and 2.73 ppm and the NOESY cross-peaks at  $\delta=3.78$  and 2.73 ppm confirm the connectivity between the CH signal (H3,3\*; new chiral center) and the CH<sub>2</sub> signals (H4,4\*; Figure 5).

**Modification of bioorthogonally functionalized somatostatin through a click reaction:** Subsequently, we investigated the opportunity to selectively address the ethynyl group of **12** in

the presence of unprotected amino acids in the somatostatin side chains. The [2+3] cycloaddition “click” reaction of an ethynyl bond with an azide functionality has been widely investigated for biological applications because this reaction can be carried out in aqueous solution at room temperature if a Cu<sup>I</sup> catalyst is added. 3-Azido-7-hydroxycoumarine was applied, which represents a profluorophore that reveals high fluorescence only after a successful “click” reaction and the formation of the triazole moiety. Therefore, this chromophore is ideally suited to verify the accessibility of bioorthogonal triple bonds of engineered biomacromolecules. By the reaction of 3-azido-7-hydroxycoumarine with ethynylsomatostatin **12**, the “click” product was obtained and the characteristic increase in fluorescence emission was observed; this reaction demonstrates selective modification of the ethynyl group (Figure 6). The successful modification was furthermore visualized and verified by gel electrophoresis and MALDI-TOF mass spectrometry, as illustrated in Figure 7. This reaction points out the value of intercalator **8** as a reagent for introducing unnatural residues that allow further chemical modifications.

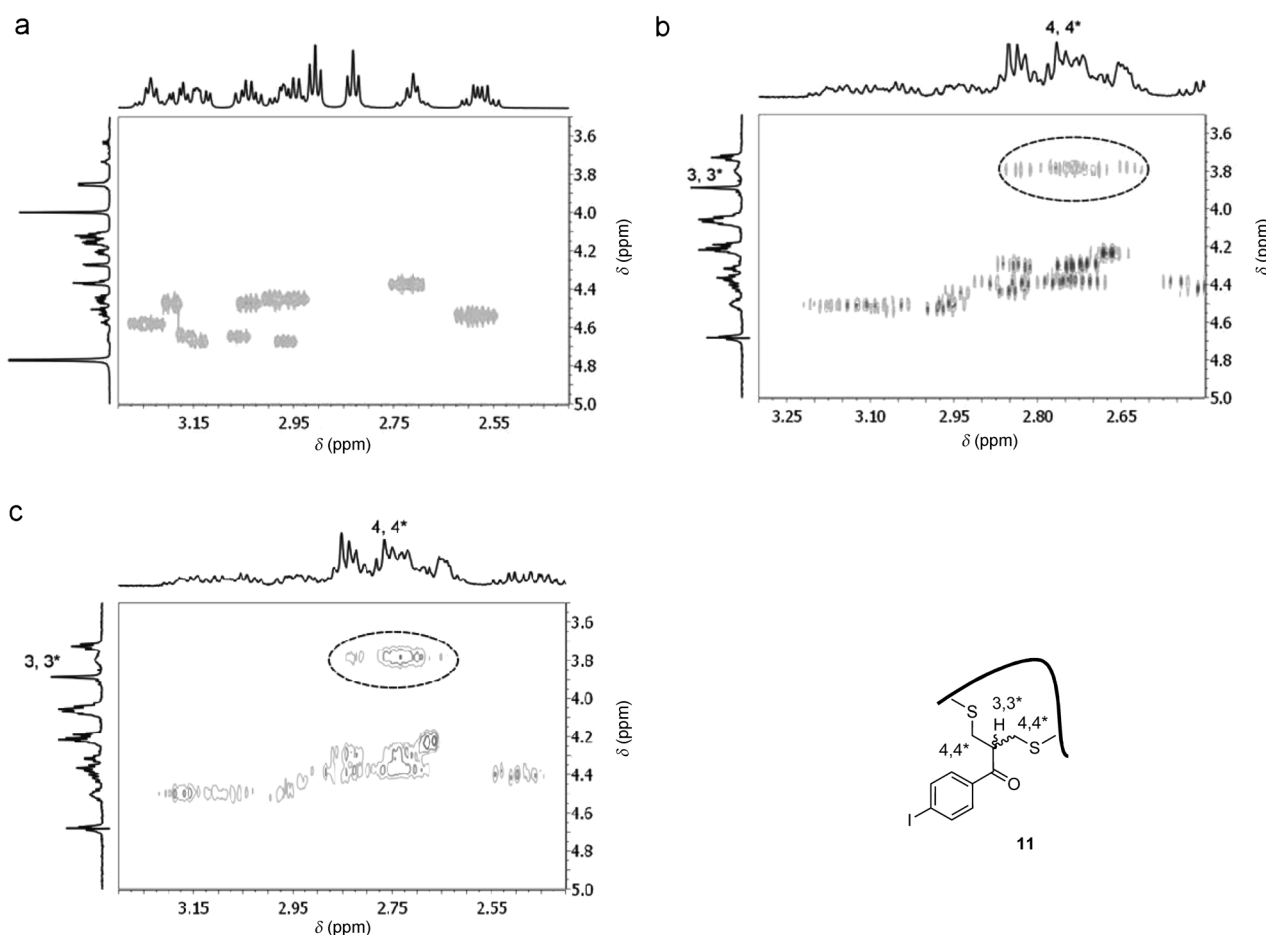


Figure 5. The cyclic geometry of **11** was proven by <sup>1</sup>H NMR spectrometry. a) <sup>1</sup>H-COSY spectrum of native somatostatin (**9**). b) <sup>1</sup>H-COSY and c) <sup>1</sup>H-NOESY spectra of iodo-modified somatostatin **11** showing cross-peaks of the signals of the newly generated methylene protons (4, 4\*) to the racemic proton (3, 3\*).

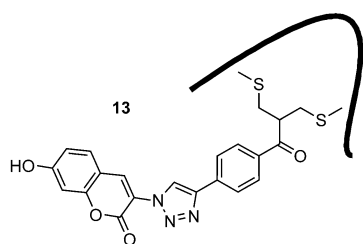
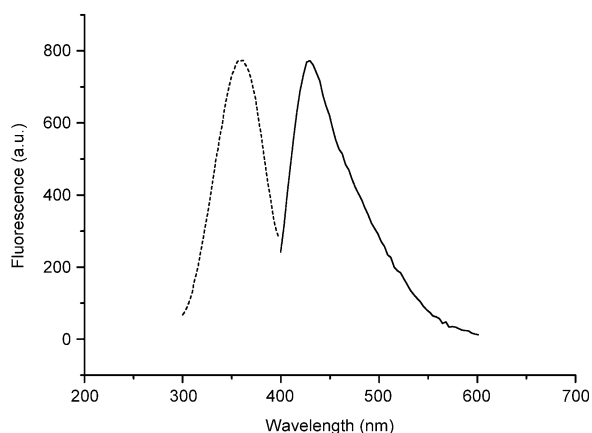


Figure 6. Absorbance (X360, —) and emission (-----) spectra of coumarin-attached somatostatin **13**.

Somatostatin–dye conjugates are particularly suitable to prove whether the biologically active 3D conformation of somatostatin was retained after modification. Even though coumarin-modified somatostatin **13** is very attractive to prove the successful cycloaddition reaction, it is also sensitive to photobleaching and does not reveal sufficient photostability for cell experiments. Therefore, the rhodamine dye intercalator **15** (Scheme 5) with increased photostability was prepared; this would allow investigation of the cell-uptake characteristics of modified somatostatin. First, commercially available lissamine rhodamine B was coupled to the active ester **14**, which was obtained by a procedure described previously.<sup>[27]</sup> Afterwards, native somatostatin was treated with the LRB intercalator **15** to yield the highly fluorescent somatostatin conjugate **16**.

**Cell uptake of modified somatostatin 16:** It has been described previously that somatostatin efficiently interacts with somatostatin G-protein-coupled receptors only in its cyclic 3D architecture. Therefore, receptor-mediated endocytosis of the representative fluorescent somatostatin derivative **16** was assessed to prove that biologically active somatostatin conjugates were achieved. CAPAN-2 cells, a human pancreas carcinoma cell line, were used as receptor-positive cells because it is known that they express somatostatin receptors that recognize somatostatin and induce its uptake. As a negative control, the A-549 cell line, which does not express somatostatin receptors, was applied. First, **16** ( $1 \text{ mg mL}^{-1}$ ) was dissolved in water in the presence of 0.1% trifluoroacetic acid (TFA) was added to the cells in culture

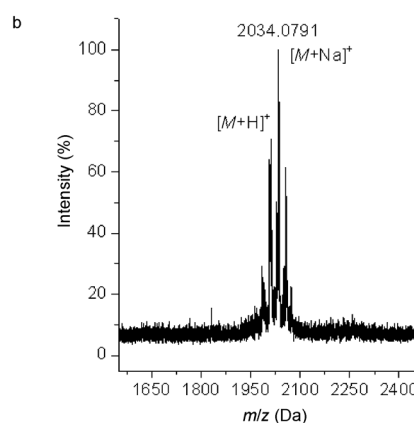
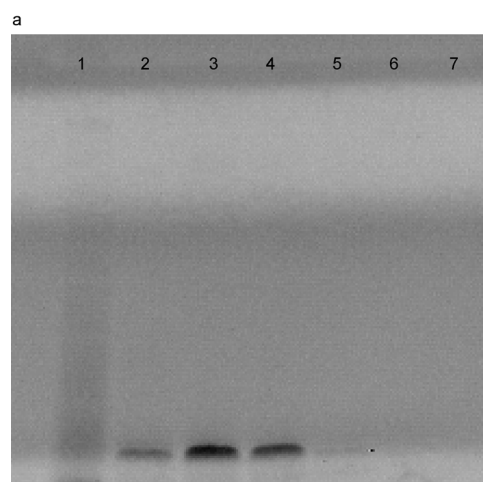
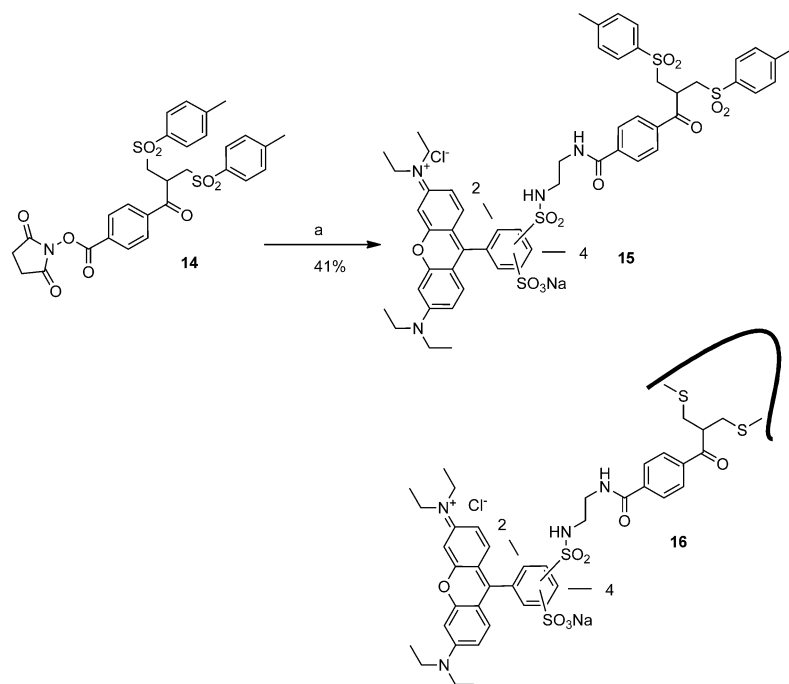


Figure 7. a) Gel electrophoresis picture taken under UV irradiation, with different concentrations of coumarin-attached somatostatin **13** (lanes 2–5) as well as native and ethynyl-modified somatostatins (lanes 6 and 7). b) MALDI-TOF mass spectrum for coumarin-attached somatostatin **13** with its salt adducts.

medium. After incubation for 24 h, the cells were washed and the cell uptake was investigated with photometric and confocal microscopy methods. In the case of A-549 cells, fluorescence staining was mainly localized at the cell membrane and no vesicles were present. By contrast, significantly increased cell uptake was clearly observed in the CAPAN-2 cells. In addition, several small vesicles were detected inside the cells, which indicates receptor-mediated cell uptake (Figure 8). These findings indicate that the biological activity of somatostatin was retained regardless of the intercalation and attachment of the large rhodamine chromophore.

Photometric investigation of cell uptake of the rhodamine-modified somatostatin in CAPAN-2 cells revealed that a dose-dependent increase in cell uptake could be detected in receptor-positive CAPAN-2 cells with increasing amounts of **16**. However, only very low emission intensities were recorded after incubation of **16** with A-549 cells, which suggests a low tendency for nonspecific cell uptake.

In order to visualize and explain these experimental results, 3D visualization of native somatostatin was achieved



Scheme 5. Synthesis of lissamine rhodamine B (LRB) bis-sulfone reagent **15**. a) Lissamine rhodamine B, dimethylformamide/dichloromethane.

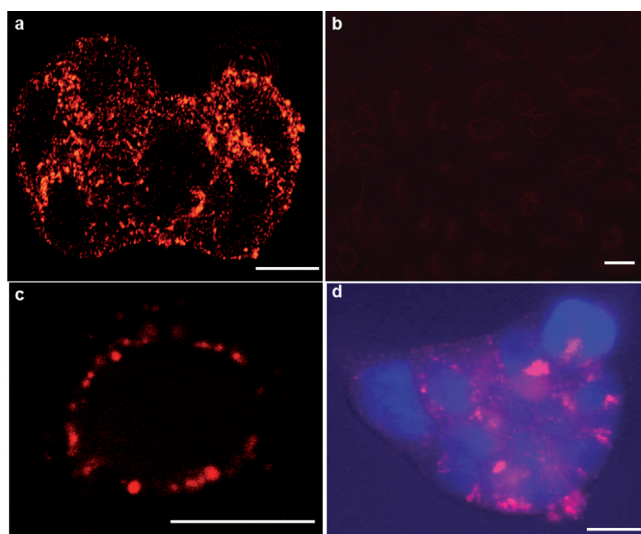


Figure 8. Confocal and fluorescence microscopy images of CAPAN-2 and A-549 cells incubated with rhodamine-modified somatostatin **16** for 24 h. a) The CAPAN-2 cell line that expresses somatostatin receptors showed an increased uptake relative to that of b) the A-549 human lung carcinoma cell line that did not express somatostatin receptors. Cells showed very weak background fluorescence. c) Clear round vesicle-like structures could be detected at a higher magnification. d) Nuclear staining with the commercially available dye DAPI showed a clear correlation between **16** and CAPAN-2 cells. White bar: 10  $\mu\text{m}$  according to magnification. Images (a–c) were recorded after laser excitation (confocal), whereas image (d) was obtained after fluorescence excitation by a mercury lamp (nonconfocal).

by applying the MOE software package of the Chemical Computing Group.<sup>[28]</sup> No crystal structure of somatostatin

has been obtained so far, so a 3D visualization of somatostatin and iodiosomatostatin **11** was achieved by connecting the respective amino acids according to the amino acid sequence, as described in the Supporting Information. The respective 3D structures are depicted in Figure 9. After intercalation of **5** into **9**, the distance between the sulphur atoms increases from about 2.1 Å to 3.9 Å, which leads to widening and, therefore, changes in the geometry near to the intercalator. However, the amino acid sequence Phe<sup>7</sup>-Trp<sup>8</sup>-Lys<sup>9</sup>-Thr<sup>10</sup> in the  $\beta$  loop of somatostatin, which is responsible for pharmacological activity, is located on the opposite side to the disulfide bridge. In comparison with the situation in native somatostatin, the distance and

orientation of the four amino acid motif remained unchanged, which is in accordance with the bioactivity data. However, according to the 3D visualization of **11**, changes

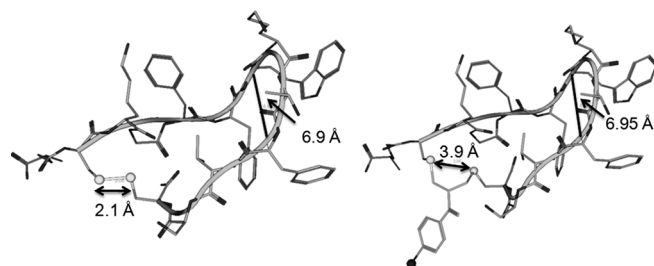
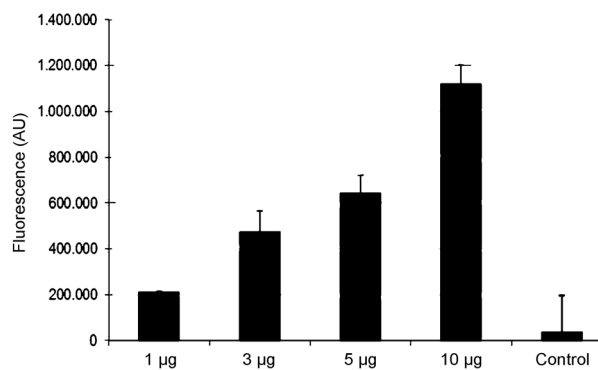


Figure 9. a) Photometric investigation of cell uptake of rhodamine-modified somatostatin **16** in CAPAN-2 cells. With increasing concentrations of **16**, increased uptake was detected in receptor-positive CAPAN-2 cells. As a control, the emission of **16** (10  $\mu\text{g}$ ) in A-549 cells was tested; very low emission was detected. 3D visualizations of b) somatostatin (**9**) and c) iodio-modified somatostatin **11**.

in the biological activity are expected if the disulfide bridge is in close vicinity to a binding motif, which should be considered if disulfide bridges are targeted by this approach.

## Conclusion

We have presented the successful synthesis of bioorthogonal conjugation reagents that facilitate the introduction of iodo and ethynyl groups into peptides by intercalation into disulfide bridges. The successful intercalation of these novel reagents was demonstrated by application to the peptide hormone somatostatin, which bears a single disulfide bridge, as a model peptide. The reaction mechanism was elucidated by 2D NMR experiments and it was shown that somatostatin diastereomers were formed due to keto–enol tautomerism of the intermediate. Both the iodo and the ethynyl group are bioorthogonal. Site-directed modification of the ethynyl-modified somatostatin and the introduction of a coumarin chromophore bearing an azido group were achieved through a [1,3] dipolar Huisgen cycloaddition reaction. The biological activity of a fluorescent somatostatin derivative bearing a single bulky rhodamine substituent was investigated in cell experiments. CAPAN-2 cells expressing somatostatin receptors revealed a high uptake of rhodamine-labeled somatostatin in a dose-dependant manner and vesicle formation indicated receptor-mediated uptake as the major pathway. By contrast, receptor-negative A-549 cells showed only very low nonspecific uptake of somatostatin conjugate **16**. The high bioactivity of **16** was explained by the retention of the bioactive conformation around the tetrapeptide receptor-binding motif and might also be due to a somewhat higher stability of the modified somatostatin in contrast to native somatostatin.

In summary, the novel bisalkylating bioconjugation agents **5** and **8** represent attractive labels for the introduction of iodo and ethynyl groups into proteins and peptides while keeping the bioactive 3D structure. Somatostatin derivatives bearing a single iodo or ethynyl group represent a valuable platform for designing an artificial somatostatin library with so-far unknown bioactivities. In addition, the attachment of further bioactive small molecules entities, such as anticancer drugs, might allow efficient and selective cell-specific delivery into cancer cells expressing somatostatin receptors. Future work will focus on increasing the solubility of **5** and **8** in aqueous media and thus facilitating their use in the absence of organic solvents; this would open up the opportunity to decorate a broad range of proteins with iodo and ethynyl groups.

## Experimental Section

Unless otherwise stated, reagents and chemicals were obtained from commercial suppliers and used without further purification. Somatostatin acetate was ordered from Chengdu CP Biochem Co., Ltd. Tris(3-hydroxypropyltriethylammonium)amine (THPTA)<sup>[29]</sup> and 4-[2',2'-bis[(4''-tolylsulfo-

nyl)methyl]acetyl]benzoic acid *N*-hydroxysuccinimide (NHS) ester (**14**)<sup>[30]</sup> were synthesized according to published procedures. The structures of the molecules were investigated on a Bruker Avance III 500 spectrometer or a Bruker Avance III 700 NMR spectrometer, both with a 5 mm  $z$ -gradient BBI <sup>1</sup>H/X probe. The proton NMR spectra were measured in D<sub>2</sub>O at 298.3 K. The temperature was kept at 298.3 K and regulated by a standard <sup>1</sup>H-methanol NMR sample. The spectra were referenced with the residual HDO signal at  $\delta(^1\text{H})=4.8$  ppm. The <sup>1</sup>H,<sup>1</sup>H 2D NOESY experiment was recorded on the 500 MHz system, with a mixing time of 0.45 s and with presaturation of the water signal during the relaxation delay and the mixing time. The <sup>1</sup>H,<sup>1</sup>H 2D COSY spectra were acquired on the 500 and 700 MHz spectrometers with presaturation on the residual water signal during relaxation delay and gradient pulses for selection.  $\pi/2$  pulse widths for <sup>1</sup>H protons of 10 and 9  $\mu\text{s}$  were chosen on the 500 and 700 MHz systems, respectively. Mass spectra were recorded in order to determine molecular weights with matrix-assisted laser desorption/ionization time-of-flight (MALDI-TOF) or field desorption (FD) mass spectrometry on Bruker Reflex and VG ZAB 2-SE-FPD Spectrofield instruments. Electrospray ionization (ESI) mass spectrometry was measured on a Navigator 1 instrument from ThermoQuest or a Finnigan MAT 95 spectrometer. Reversed-phase chromatography purification was performed on a Resource RPC 3 mL column from GE Healthcare at a flow rate of 2 mL min<sup>-1</sup> with a linear gradient of buffer B (0–60% over 8 min and 60–100% over 6.5 min) in buffer A (buffer A: 0.1% TFA in H<sub>2</sub>O; buffer B: 0.1% TFA in CH<sub>3</sub>CN). HPLC purification was performed on a Jasco HPLC 2000 series system at a flow rate of 10 mL min<sup>-1</sup> with a linear gradient of buffer B (10% for 3 min, 10–70% over 21 min, 70–100% over 0.5 min, and 100% for 9.5 min) in buffer A (buffer A: 0.1% TFA in H<sub>2</sub>O; buffer B: 0.1% TFA in 95% CH<sub>3</sub>CN).

Detailed descriptions of the syntheses of 1-[3'-(4''-iodophenyl)-3'-oxopropyl]piperidinium hydrochloride (**2**), 2,2-bis[(4''-tolylthio)methyl]-4'-iodoacetophenone (**3**), and 2,2-bis[(4''-tolylthio)methyl]-4'-trisopropylsilylthioacetophenone (**6**) can be found in the Supporting Information.

**2,2-Bis[(4''-tolylsulfonyl)methyl]-4'-iodoacetophenone (4):** Iodo-bis-sulfide **3** (0.2 g, 0.4 mmol) and potassium peroxomonosulfate (0.95 g, 1.54 mmol) were suspended in EtOAc/CH<sub>3</sub>CN/H<sub>2</sub>O (6:6:1, 8 mL). The reaction mixture was stirred at ambient temperature overnight. The solution was filtered and diluted with ethanol/water (1:1, 100 mL) and then the aqueous phase was washed twice with ethyl acetate (50 mL). The organic solution was dried with magnesium sulphate. Gravity filtration followed by removal of volatiles gave **4** as a colorless solid product: yield: 0.21 g (90%); <sup>1</sup>H NMR (300 MHz, CDCl<sub>3</sub>, tetramethylsilane (TMS)):  $\delta=7.76$  (d,  $J=8.6$  Hz, 2H), 7.72 (d,  $J=8.3$  Hz, 4H), 7.40–7.25 (m, 6H), 4.33 (quintet,  $J=6.3$  Hz, 1H), 3.55 (qd,  $J=14.3$ , 6.3 Hz, 4H), 2.50 ppm (s, 6H); <sup>13</sup>C NMR (75 MHz, CDCl<sub>3</sub>):  $\delta=200.09$ , 145.49, 138.24, 137.63, 135.39, 130.16, 129.81, 128.33, 112.02, 55.68, 21.72 ppm; FT-IR:  $\tilde{\nu}=740$ , 802, 868, 928, 1000, 1020, 1090, 1140, 1170, 1200, 1240, 1300, 1390, 1420, 1490, 1580, 1680, 2910, 2980, 3020, 3090 cm<sup>-1</sup>; UV/Vis (acetonitrile):  $\lambda_{\text{max}}$  ( $\epsilon$ )=225 (14210), 274 nm (3877 mol<sup>-1</sup>dm<sup>3</sup>cm<sup>-1</sup>); FD MS:  $m/z$ : 581.8 [M]<sup>+</sup>; HRMS (ESI): calcd: 604.9929; found: 604.9958.

**2-[(4''-Tolylsulfonyl)methyl]-3-(4'-iodophenyl)-3-oxo-prop-1-ene (5):** Potassium *tert*-butoxide (0.076 g, 0.68 mmol) was dissolved in tetrahydrofuran (34 mL). Iodo-bis-sulfone **4** (0.1 g, 0.17 mmol) was dissolved in tetrahydrofuran (10 mL) and slowly added to the first solution. The resulting mixture was stirred at ambient temperature for 1 hour. The solution was diluted with dichloromethane/water (1:1, 100 mL), extracted with dichloromethane, and dried with magnesium sulfate. After filtration, drying in vacuo gave **5** as colorless solid and the crude product was purified by chromatography (silica gel, hexane/acetone 3:1): yield: 0.052 g (72%); <sup>1</sup>H NMR (250 MHz, CD<sub>2</sub>Cl<sub>2</sub>, TMS):  $\delta=7.83$  (d,  $J=8.4$  Hz, 2H), 7.75 (d,  $J=8.3$  Hz, 2H), 7.40 (d,  $J=8.4$  Hz, 2H), 7.34 (d,  $J=8.2$  Hz, 2H), 6.14 (s, 1H), 5.94 (s, 1H), 4.31 (s, 2H), 2.41 ppm (s, 3H); <sup>13</sup>C NMR (75 MHz, TMS):  $\delta=194.30$ , 145.64, 138.03, 136.28, 136.13, 136.07, 133.94, 131.36, 130.25, 128.64, 100.51, 58.23, 21.75 ppm; FT-IR:  $\tilde{\nu}=665$ , 710, 789, 839, 899, 987, 1090, 1150, 1250, 1290, 1400, 1480, 1580, 1650, 2380, 2980 cm<sup>-1</sup>; UV/Vis (acetonitrile):  $\lambda_{\text{max}}$  ( $\epsilon$ )=271 (24400), 225 nm (6000 mol<sup>-1</sup>dm<sup>3</sup>cm<sup>-1</sup>); FD MS:  $m/z$ : 425.4 [M]<sup>+</sup>; HRMS (ESI): calcd: 448.9684; found: 448.9691.

**2-[(4'-Tolylsulfonyl)methyl]-3-(4'-ethynylphenyl)-3-oxo-prop-1-ene (8):** TIPS-protected ethynyl-bis-sulfone (**6**; 0.105 g, 0.18 mmol) and oxone (0.443 g, 0.72 mmol) were suspended in dichloromethane (10 mL). The suspension was allowed to stir at ambient temperature for 24 h and afterwards filtered to take out the salts. The volatiles were removed in vacuo and the residue was dissolved in dry THF (10 mL). TBAF (0.094 g, 0.36 mmol) was added to the solution and, after 10 min of stirring, the reaction was quenched by adding water (10 mL). The aqueous phase was extracted twice with dichloromethane (20 mL) and the combined organic solutions were dried with magnesium sulphate. After filtration and removal of the volatiles in vacuo, the crude product was purified by chromatography (silica gel, hexane/acetone 3:1): yield: 0.041 g (70%); <sup>1</sup>H NMR (250 MHz, CD<sub>2</sub>Cl<sub>2</sub>, TMS): δ = 7.75 (d, *J* = 8.3 Hz, 2H), 7.64 (d, *J* = 8.6 Hz, 2H), 7.54 (d, *J* = 8.6 Hz, 2H), 7.35 (d, *J* = 8.6 Hz, 2H), 6.15 (s, 1H), 5.95 (s, 1H), 4.31 (s, 2H), 3.32 (s, 7H), 2.41 ppm (s, 3H); <sup>13</sup>C NMR (75 MHz, TMS): δ = 193.97, 136.06, 135.96, 135.75, 133.80, 131.97, 129.85, 129.55, 128.34, 126.55, 107.54, 82.64, 80.29, 57.84, 21.62 ppm; FT-IR:  $\tilde{\nu}$  = 665, 710, 789, 839, 899, 987, 1090, 1150, 1250, 1290, 1400, 1480, 1580, 1650, 2380, 2980 cm<sup>-1</sup>; UV/Vis (acetonitrile):  $\lambda_{\text{max}}$  ( $\epsilon$ ) = 271 (24400), 225 nm (6000 mol<sup>-1</sup> dm<sup>3</sup> cm<sup>-1</sup>); FD MS: *m/z*: 323.4 [*M*]<sup>+</sup>; HRMS (ESI): calcd: 325.0898; found: 325.0908.

**LRB intercalating agent (15):** 4-[2',2'-Bis[(4'-tolylsulfonyl)methyl]acetyl]-benzoic acid NHS ester (**14**; 17 mg, 0.034 mmol) and LRB (10 mg, 0.017 mmol) were dissolved in dichloromethane (3 mL) and dimethylformamide (1 mL). The solution was allowed to stir at ambient temperature for 72 h and afterwards was directly loaded on an aluminium oxide column and eluted with ethyl acetate/ethanol (1:1). After removal of the volatiles in vacuo, the residue was redissolved in a small quantity of acetone and the product was precipitated into hexanes: yield: 7.5 mg (41%); MALDI-TOF MS: *m/z*: 1083.42 [*M*]<sup>+</sup>.

**Iodo-modified somatostatin (11):** Somatostatin acetate (**9**; 5 mg, 3 μmol) was dissolved in 0.05 M sodium phosphate at pH 7.8 (12 mL). Tris(2-carboxyethyl)phosphine HCl (1.7 mg, 6 μmol) was added and the solution was incubated at room temperature for 30 min. Iodomonosulfone **5** (3.5 mg, 6 μmol) was dissolved in acetonitrile (8 mL) and slowly added to the first solution. The resulting mixture was incubated at ambient temperature for 24 h, concentrated in vacuo, and filtered through a membrane filter (0.22 μm). The modified peptide was obtained after purification by reversed-phase chromatography and freeze-drying of the pooled fractions: yield: 43% (gravimetric determination after HPLC purification); MALDI-TOF MS: *m/z*: 1909.5 [*M*]<sup>+</sup>; HRMS (ESI-TOF): calcd: 1909.6987; found: 1909.6993.

**Ethynyl-modified somatostatin (12):** The preparation and purification were carried out in the same way as for the synthesis of **11**; for the modification, ethynylmonosulfone **8** (2 mg, 6 μmol) was added in acetonitrile (8 mL): yield: 56% (gravimetric determination after HPLC purification); MALDI-TOF MS: *m/z*: 1809.24 [*M* + H]<sup>+</sup>.

**Coumarin-modified somatostatin (13):** Ethynyl-modified somatostatin **8** (0.05 mg, 0.03 μmol) was dissolved in H<sub>2</sub>O (90 μL) and 0.05 M sodium phosphate (pH 7.8; 298 μL) was added. 3-Azido-7-hydroxycoumarin (0.01 mg, 0.05 μmol) in dimethylsulfoxide (50 μL) was added to this mixture. Copper sulphate (0.008 mg, 0.05 μmol) in H<sub>2</sub>O (2.3 μL) was pre-mixed with tris(3-hydroxypropyl)trimethylamine (0.11 mg, 0.25 μmol) in deionized water (34.3 μL) and then added to the reaction solution. After addition of aminoguanidine (0.19 mg, 2.5 μmol) in water (4.8 μL) and sodium ascorbate (0.5 mg, 2.5 μmol) in water (34.3 μL), the mixture was mixed and incubated at ambient temperature for 24 h, concentrated in vacuo, and filtered through a membrane filter with 0.22 μm pore size. Modified peptide **13** was obtained after purification by reversed-phase chromatography and freeze-drying of the pooled fractions: MALDI-TOF MS: *m/z*: 2012.09 [*M* + H]<sup>+</sup>.

**LRB-modified somatostatin (16):** Somatostatin acetate (**9**, 1 mg, 0.6 μmol) was dissolved in 0.05 M sodium phosphate at pH 7.8 (2.4 mL). Tris(2-carboxyethyl)phosphine hydrochloride (0.34 mg, 6 μmol) was added and the solution was incubated at room temperature for 30 min. LRB-bis-sulfone (**15**; 3.25 mg, 3 μmol) was dissolved in acetonitrile (1.6 mL) and slowly added to the first solution. The resulting mixture was incubated at ambient temperature for 24 h, concentrated in vacuo,

and filtered through a 0.22 μm membrane filter. The modified peptide was obtained after purification by reversed-phase chromatography and freeze-drying of the pooled fractions: MALDI-TOF MS: *m/z*: 2412.11 [*M*]<sup>+</sup>.

A detailed description of the visualization of somatostatin derivative **11** in comparison to somatostatin and the experimental details of the cell-culture experiments can be found in the Supporting Information.

## Acknowledgements

Financial support from the DFG (SFB 625) is gratefully acknowledged.

- [1] U. B. Kompella, V. H. L. Lee in *Peptide and Protein Drug Delivery* (Ed.: V. H. L. Lee), Marcel Dekker, New York, **1991**, pp. 391–484.
- [2] J. M. Harris, R. B. Chess, *Nat. Rev. Drug Discov.* **2003**, *2*, 214–221.
- [3] P. Caliceti, F. M. Veronese, *Adv. Drug Delivery Rev.* **2003**, *55*, 1261–1277.
- [4] H. B. F. Dixon, *J. Protein Chem.* **1984**, *3*, 99–108.
- [5] H. Lee, I. H. Jang, S. H. Ryu, T. G. Park, *Pharm. Res.* **2003**, *20*, 818–825.
- [6] O. Kinstler, G. Molineux, M. Treuheit, D. Ladd, C. Gegg, *Adv. Drug Delivery Rev.* **2002**, *54*, 477–485.
- [7] L. Polgar, M. L. Bender, *J. Am. Chem. Soc.* **1966**, *88*, 3153–3154.
- [8] P. I. Clark, G. Lowe, *J. Chem. Soc. Chem. Commun.* **1977**, 923–924.
- [9] G. J. L. Bernardes, J. M. Chalker, J. C. Errey, B. G. Davis, *J. Am. Chem. Soc.* **2008**, *130*, 5052.
- [10] T. H. Yoo, D. A. Tirrell, *Angew. Chem.* **2007**, *119*, 5436–5439; *Angew. Chem. Int. Ed.* **2007**, *46*, 5340–5343.
- [11] A. J. Link, M. L. Mock, D. A. Tirrell, *Curr. Opin. Biotechnol.* **2003**, *14*, 603–609.
- [12] S. Mitra, R. G. Lawton, *J. Am. Chem. Soc.* **1979**, *101*, 3097–3110.
- [13] S. Balan, J.-W. Choi, A. Godwin, I. Teo, C. M. Laborde, S. Heidelberger, M. Zloh, S. Shaunak, S. Brocchini, *Bioconjugate Chem.* **2007**, *18*, 61–76.
- [14] S. W. J. Lamberts, E. P. Krenning, J. C. Reubi, *Endocr. Rev.* **1991**, *12*, 450–482.
- [15] M. N. Pollak, A. V. Schally, *Proc. Soc. Exp. Biol. Med.* **1998**, *217*, 143–152.
- [16] A. V. Schally, A. Nagy, *Eur. J. Endocrinol.* **1999**, *141*, 1–14.
- [17] M. C. De Martino, L. J. Hofland, S. W. Lamberts, *Prog. Brain Res.* **2010**, *182*, 255–280.
- [18] A. Otte, J. Mueller-Brand, S. Dellas, E. U. Nitzsche, R. Herrmann, H. R. Maecke, *Lancet* **1998**, *351*, 417–418.
- [19] W. W. de Herder, L. J. Hofland, A. J. van der Lely, S. W. J. Lamberts, *Endocr.-Relat. Cancer* **2003**, *10*, 451–458.
- [20] J. M. Beierle, W. S. Horne, J. H. van Maarseveen, B. Waser, J.-C. Reubi, M. R. Ghadiri, *Angew. Chem.* **2009**, *121*, 4819–4823; *Angew. Chem. Int. Ed.* **2009**, *48*, 4725–4729.
- [21] A. V. Schally, A. M. Comaru-Schally in *Cancer Medicine*, 4th ed. (Eds.: R. Holland, E. Frei III, R. R. Bast, Jr, D. E. Kufe, D. L. Morton, R. R. Weichselbaum), Williams and Wilkins, Baltimore, **1997**, pp. 1067–1086.
- [22] W. Bauer, U. Briner, W. Doepfner, R. Haller, R. Huguenin, P. Marbach, T. J. Petcher, J. Pless, *Life Sci.* **1982**, *31*, 1133–1140.
- [23] R. Z. Cai, B. Szoke, R. Lu, D. Fu, T. W. Redding, A. V. Schally, *Proc. Natl. Acad. Sci. USA* **1986**, *83*, 1896–1900.
- [24] A. V. Schally, *Cancer Res.* **1988**, *48*, 6977–6985.
- [25] M. A. Gauthier, H. A. Klok, *Chem. Commun.* **2008**, 2591–2611.
- [26] F. A. Liberatore, R. D. Corneau, J. M. McKearin, D. A. Pearson, B. Q. Belonga III, S. J. Brocchini, J. Kath, T. Phillips, K. Oswell, R. G. Lawton, *Bioconjugate Chem.* **1990**, *1*, 36–50.
- [27] S. Brocchini, S. Balan, A. Godwin, J.-W. Choi, M. Zloh, S. Shaunak, *Nat. Protoc.* **2006**, *1*, 2241–2252.
- [28] The Molecular Operating Environment (MOE) 2009.10, Chemical Computing Group Inc., Montreal, QC (Canada); available at <http://www.chemcomp.com>

[29] T. R. Chan, R. Hilgraf, K. B. Sharpless, V. V. Fokin, *Org. Lett.* **2004**, *6*, 2853–2855.

[30] S. Shaunak, A. Godwin, J.-W. Choi, S. Balan, E. Pedone, D. Vijayarangam, S. Heidelberger, I. Teo, M. Zloh, S. Brocchini, *Nat. Chem. Biol.* **2006**, *2*, 312–313.

Received: January 26, 2011

Revised: April 26, 2011

Published online: July 11, 2011